Assembly of *Agrobacterium* Phytochromes Agp1 and Agp2 with Doubly Locked Bilin Chromophores[†]

Katsuhiko Inomata,*[,‡] Htoi Khawn,[‡] Li-Yi Chen,[‡] Hideki Kinoshita,[‡] Benjamin Zienicke,[§] Isabel Molina,[§] and Tilman Lamparter*[,§]

Division of Material Sciences, Graduate School of Natural Science and Technology, Kanazawa University, Kakuma, Kanazawa, Ishikawa 920-1192, Japan, and Universität Karlsruhe, Botanik I, Kaiserstrasse 2, D-76131 Karlsruhe, Germany

Received December 22, 2008; Revised Manuscript Received January 28, 2009

ABSTRACT: The natural chromophore of most bacterial and fungal phytochromes is biliverdin (BV), which is incorporated in a covalent manner into the protein. Upon photoconversion between the red light-absorbing form Pr and the far-red light-absorbing form Pfr, the stereochemistry of the chromophore around the C15 methine bridge changes from *Z anti* to *E anti*. Recombinant phytochromes Agp1 and Agp2 from *Agrobacterium tumefaciens* were assembled with a set of synthetic chromophores, including 2,18-Et-BV, 3,18-Et-BV, and the doubly locked 5*Ea*15*Ea*-BV, 5*Es*15*Ea*-BV, 5*Za*15*Ea*-BV, and 5*Zs*15*Ea*-BV. In all chromophores, covalent bond formation is restricted. As shown by spectral changes and desalting column separation, all chromophores are bound to Agp1 and Agp2. Adducts with 2,18-Et-BV and 3,18-Et-BV undergo normal photoconversion between Pr and Pfr. As opposed to typical phytochromes, the BV−Agp2 adduct converts from Pr to Pfr in darkness. However, the 2,18-Et-BV−Agp2 and 3,18-Et-BV−Agp2 adducts can undergo dark conversion from Pr to Pfr and Pfr to Pr, showing that ring A of the chromophore has a direct impact on the direction of dark conversion. The doubly locked chromophores were designed to probe for the stereochemistry of the C5 methine bridge in the Pfr form. The adducts with 5*Es*15*Ea*-BV and 5*Zs*15*Ea*-BV absorbed in the blue spectral range only. Therefore, the C5 *E syn* and *Z syn* stereochemistries are unlikely for the Pfr chromophore of Agp1 and Agp2. According to our spectra, the Agp2 chromophore most likely adopts an *E anti* stereochemistry at its C5 methine bridge. Thus, during Pr to Pfr conversion, the C5 methine bridge of the chromophore might undergo a Hula-twist isomerization. In Agp1, the Pfr chromophore is most likely in the C5 *Z anti* stereochemistry. We propose that the stereochemistry of the C5 methine bridge might differ between different phytochromes, most particularly in the Pfr form.

Phytochromes are photoreceptors that have been identified in plants, where they mediate a large number of light responses (*1, 2*). Plant phytochromes carry one phytochromobilin chromophore per protein subunit, which covalently attaches to a conserved Cys residue (*3*). Chromophore incorporation results in the formation of Pr,[1] the red light-absorbing form of phytochrome. Light absorbed by Pr triggers photoconversion into far-red light-absorbing form Pfr, a process during which the absorption maximum is bathochromically shifted by 40−70 nm (*4*). The photoconversion of Pfr results in the formation of Pr, completing the photocycle.

Due to the tremendous increase in the amount of DNA sequence information over the past decade, many phytochrome genes have been found in cyanobacteria, other bacteria, and fungi (*5*−*7*). An increasing number of these microbial phytochromes are being characterized as recombinant proteins. In most cases, these bacterial and fungal phytochromes share the photoreversibility of plant phytochromes, i.e., undergo reversible photoconversion between two spectrally different forms Pr and Pfr. Although the domain arrangement of phytochromes varies, there is a typical widespread pattern: the N-terminus carries PAS, GAF, and PHY domains, and the C-terminus bears a histidine kinase related domain (*4*). The PAS, GAF, and PHY domains in the N-terminus are required for the incorporation of the chromophore and photoreversibility. A separate N-terminal extension is found in plant and fungal phytochromes (*7*).

The most ancient phytochrome chromophore is probably biliverdin (BV), which is synthesized in vivo by oxygenation from heme. This chromophore is used in most bacterial phytochromes and in fungi (*8, 9*). Cyanobacterial phytochromes can carry BV (*10*) as a chromophore or phycocyanobilin (*11*), which is also the dominant chromophore of the light-harvesting phycobiliproteins. Biliverdin (BV) binding phytochromes use a cysteine in the PAS domain as the

[†] This work was financially supported by a Grant-in-Aid for Scientific Research (B) (19350082) from the Japan Society for the Promotion of Science (JSPS) (to K.I.) and by Deutsche Forschungsgemeinschaft Grant Sfb 498, B2 (to T.L.).

* To whom correspondence should be addressed. K.I.: e-mail, inomata@cacheibm.s.kanazawa-u.ac.jp; phone, +81-76-264-5700; fax, +81-76-264-5742. T.L.: e-mail, tilman.lamparter@kit.edu; phone, +49(0)7216085441; fax, +49(0)7216084193.

[‡] Kanazawa University.

[§] Universität Karlsruhe.

[1] Abbreviations: *a*, *anti* conformation; BV, biliverdin; C5, carbon atom at position 5 of biliverdin; Pr, red light-absorbing form of phytochrome; Pfr, far-red light-absorbing form of phytochrome; *s*, *syn* conformation.

10.1021/bi802334u CCC: $40.75
Published on Web 01/30/2009

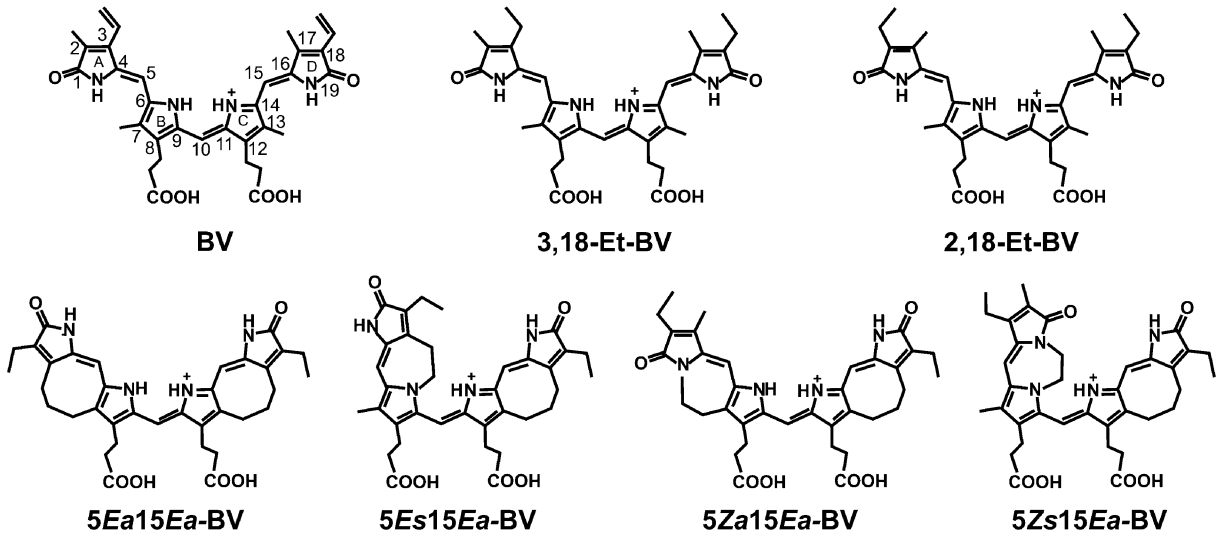

FIGURE 1: Chromophores used in this study. The natural chromophore biliverdin (BV) is shown for comparison.

chromophore binding site (*12, 13*), whereas the chromophore binding Cys residue of phycocyanobilin and phytochromobilin binding phytochromes lies within the GAF domain.

Although both Pr and Pfr are "quite" stable, slow dark conversion from Pfr to Pr has been found and characterized for plant phytochromes in vivo and in vitro (*14*). In plants, dark conversion is one of several possibilities for inactivating phytochrome. In the soil bacterium *Agrobacterium tumefaciens*, two phytochromes termed Agp1 and Agp2 or AtBphP1 and AtBphP2 have been found and characterized (*12, 15*−*24*). Agp1 converts also from Pfr to Pr in darkness and thus resembles plant phytochromes in this respect. In contrast, Agp2 converts in darkness from Pr to Pfr. This reversed dark conversion behavior was found for some other bacterial phytochromes as well (*25, 26*). Phytochromes with reversed dark conversion are termed bathy-phytochromes.

The spectral properties of the chromophore within the holoprotein are determined by the conjugated double bond system. For a given bilin chromophore, stereochemistry, torsions around methine bridges, protonation status, and interactions with particular amino acids might play important roles in determining the spectral properties. Insight into the structure of the Pr and Pfr chromophore has been gained from vibrational spectroscopy (*27*−*30*), X-ray analyses (*31*−*34*), and NMR studies (*35*−*39*) on recombinant phytochromes. The stereochemistry in the Pr and Pfr forms has also been addressed by studies with synthetic locked chromophores (*18, 19, 40*). It is still a central open question why phytochromes undergo a large bathochromic shift during Pr to Pfr photoconversion. The high-resolution crystal structure of a phytochrome fragment of *Deinococcus radiodurans* BphP (DrBphP) in the Pr state revealed a *Z syn Z syn Z anti* stereochemistry for the Pr chromophore (*41*). The same stereochemistry was confirmed for the Pr chromophores of *Rhodopseudomonas* BphP3 (RpBphP3) (*31*) and cyanobacterial phytochrome Cph1 (*34*). Most recent vibrational and NMR spectroscopy supported this view, although spectra have previously also been interpreted in different manners (*28*). Upon photoconversion to Pfr, a *Z* to *E* isomerization around the ring C−D connecting methine bridge takes place, whereas the single bond remains in the *anti* conformation. The recently published crystal structure of *Pseudomonas aeruginosa* BphP (PaBphP) which is in the Pfr form is in agreement with an *E anti* stereochemistry of the C−D connecting methine bridge, but the resolution leaves place for other interpretations (*32*). According to this crystal structure, the stereochemistry of the three methine bridges in the Pfr form is identical to that of the Pr chromophores except the configuration of the C15═C16 bond. NMR spectroscopy with cyanobacterial phytochrome Cph1 in which the chromophore was labeled with ^{15}N and ^{13}C also provided evidence that only the stereochemistry of the C15═C16 bond is changed and that the stereochemistry of other methine bridges remains unchanged (*35, 39*).

In the first studies with locked chromophores, the stereochemistry of the C15 methine bridge (the ring C−D connecting methine bridge; see Figure 1) has been addressed. A set of four chromophores, in which this methine bridge is fixed in all possible conformations and/or configurations, have been assembled with Agp1 (*19*) and Agp2 (*18*). These locked chromophores are termed 15*Za*, 15*Zs*, 15*Ea*, and 15*Es*, according to the number of the locked C methine atom, the configuration of the double bond (*Z* or *E*), and the conformation of the single bond (*syn* or *anti*). All locked chromophores were incorporated into the chromophore pocket of Agp1 and Agp2 and covalently bound to the protein. The spectra of the 15*Za* and 15*Ea* adducts resembled the spectra of Pr and Pfr, respectively. From these facts, we concluded that the double bond undergoes a *Z* to *E* isomerization during the photoconversion from Pr to Pfr, whereas the single bond remains in the *anti* conformation throughout the photocycle. The *Z* to *E* isomerization has long been proposed for plant phytochromes (*42*), whereas the status of the single bond during photoconversion has been controversially discussed. The adducts with the locked chromophores are photoinactive. Thus, these results confirmed the assumption that isomerization around the C15═C16 bond is the first step in the photocycle, for both Pr to Pfr and Pfr to Pr photoconversion. The 15*Zs* and 15*Es* adducts absorb in the blue spectral region only. It has been proposed that either the C10═C11 bond of the "15-*syn* chromophores"

is lost upon interaction with the protein or the conjugated system is interrupted because a kink is formed between rings B and C.

The stereochemistry of the C5 methine bridge has been probed by two synthetic chromophores termed 5*Za* and 5*Zs*. Both chromophores were also incorporated into Agp1 and Agp2 in a covalent manner (*18*). The absorption maxima of the adducts were in the region of the corresponding Pr form, but the absorption maximum of the 5*Zs* adduct matched better than that of the 5*Za* adduct. It was thus concluded that the Pr chromophore has a C4═C5 *Z* configuration and a C5−C6 *syn* conformation, in line with the crystal structures of DrBphP and RpBphP3. Irradiation of the 5*Zs* and 5*Za* adducts induced spectral changes. However, the 5*Zs* adducts shifted to shorter wavelengths (*18*). In flash photolysis experiments, 5*Zs*-Agp1 revealed only rapidly formed intermediates (*40*), suggesting that the later steps of Pfr formation are missing because of the missing flexibility of the C5 methine bridge. This interpretation predicts that the stereochemistry of the C5 methine bridge is altered upon photoconversion, in contrast to the NMR data on Cph1 (*35, 39*) and the crystal structure of PaBphP in the Pfr form (*32*).

It is possible that during Pr to Pfr conversion, the C15 isomerization must precede the proposed changes around the C5 methine bridge. Moreover, the 5*Ea* and 5*Es* stereochemistry has as yet not been tested with locked chromophores. We therefore tested doubly locked chromophores in which the C15 methine bridge has an *Ea* stereochemistry, as in Pfr, and the C5 methine bridge is locked in either *Ea*, *Es*, *Za*, or *Zs*. Although these chromophores do not covalently attach to the protein due to missing a vinyl group at the C3 position, they are incorporated into Agp1 and Agp2 and revealed characteristic absorption spectra. The most likely candidate for a Pfr chromophore is 5*Ea*15*Ea*-BV which formed a Pfr-like adduct with the Agp2 apoprotein.

MATERIALS AND METHODS

UV−Vis Spectroscopy. All UV−vis measurements were performed in a JASCO V-550 photometer at 20 °C.

Protein Purification. A. tumefaciens strain C58 full-length phytochromes Agp1 and Agp2 were expressed as poly-His-tagged proteins in *Escherichia coli* and purified by Ni affinity chromatography as described previously (*18*). The pure apoproteins were dissolved in "basic buffer" which consists of 50 mM Tris-HCl, 300 mM NaCl, and 5 mM EDTA (pH 7.8). All assembly experiments were performed in this buffer. In general, the concentration of the apoprotein was adjusted to an A_{280} of 1, which is equivalent to a concentration of 10 μM for Agp1 and 12 μM for Agp2.

Chromophores and Chromophore Synthesis. The doubly locked chromophores 5*Ea*15*Ea*-BV, 5*Es*15*Ea*-BV, 5*Za*15*Ea*-BV, and 5*Zs*15*Ea*-BV (see Figure 1) were synthesized as described previously (*43*). The synthesis of 3,18-Et-BV is described in refs *15* and *44*, and 2,18-Et-BV was synthesized in a similar manner. Biliverdin (BV) was obtained from Frontier Scientific. All chromophores were dissolved in DMSO at concentrations of ca. 4 mM. The exact concentrations of the stock solutions were estimated by measuring the absorption spectra of diluted samples in methanol-HCl. Reference spectra had been obtained under identical conditions for all chromophores directly after synthesis (*43*).

Chromophore Assembly. The final chromophore concentration was either 5 or 10 μM. Assembly was initiated by adding a chromophore stock solution (ca. 2−3 μL, depending on the exact concentration of the stock solution) to 1 mL of a protein solution at 20 °C and mixing the sample rapidly with a pipet. Immediately thereafter, an absorption spectrum was measured from 250 to 900 nm. The time between chromophore addition and the first spectrum is typically 1 min for the measurement in the red spectral region. Note that the complete scan takes ca. 1 min and that the measurements proceed from longer to shorter wavelengths. To follow the incorporation of the chromophores kinetically, absorption spectra were subsequently recorded in 3 or 10 min intervals for up to 120 min or until no further absorbance changes were observed. Information from these spectra was used to describe the kinetics of assembly for each chromophore.

NAP Column Separation. For the separation of protein from the free chromophore, samples were passed through desalting columns (NAP-10 columns, GE Healthcare; called NAP columns herein) which are designed to desalt 1 mL of sample. The columns were equilibrated with basic buffer. For the separation, 1 mL of holoprotein solution was applied to the column and the flow through was discarded. Thereafter, 1.5 mL of basic buffer was applied and the flow through, which contains the protein, was collected. Free chromophore is not eluted because of the low molecular weight and because free bilins interact strongly with the column matrix (*12*). Spectra were recorded before and after the separation. To compensate for the dilution, both spectra were normalized to A_{280}.

RESULTS

Chromophores and Proteins. This work concentrates on the assembly of Agp1 and Agp2 with synthetic chromophores, which have two locked dipyrrole components (*43*). These chromophores are termed 5*Ea*15*Ea*-BV, 5*Es*15*Ea*-BV, 5*Za*15*Ea*-BV, and 5*Zs*15*Ea*-BV (see Figure 1). All four chromophores have one common terminal methine bridge fixed in the *E anti* form, thereby reflecting the stereochemistry of the C15 methine bridge of the Pfr chromophore. The other terminal methine bridge is locked in one of all four possible forms. The natural chromophore biliverdin (BV) has vinyl side chains at the C3 and C18 positions and methyl groups at the C2 and C17 positions. The double bond of the 3-vinyl group is required for the formation of a covalent bond with the protein (*15*). For technical reasons, both vinyl side chains are replaced with ethyl groups in the locked chromophores and are positioned at C2 and C18 in 5*Ea*15*Ea*-BV, 5*Es*15*Ea*-BV, and 5*Za*15*Ea*-BV, whereas 5*Zs*15*Ea*-BV has ethyl side chains at the C3 and C18 positions. Because they are missing the double bond at the C3 position, all locked chromophores will not form a covalent link with the protein. For Agp1 and other phytochromes, it has been shown that the covalent bond is required neither for the proper incorporation into the chromophore pocket of the protein nor for Pr to Pfr photoconversion, although noncovalent and covalent adducts exhibit subtle spectral differences (*12, 15*).

As control chromophores, we used the synthetic BV derivatives 2,18-Et-BV and 3,18-Et-BV (Figure 1). The 3,18-Et-BV chromophore has already been tested for its assembly

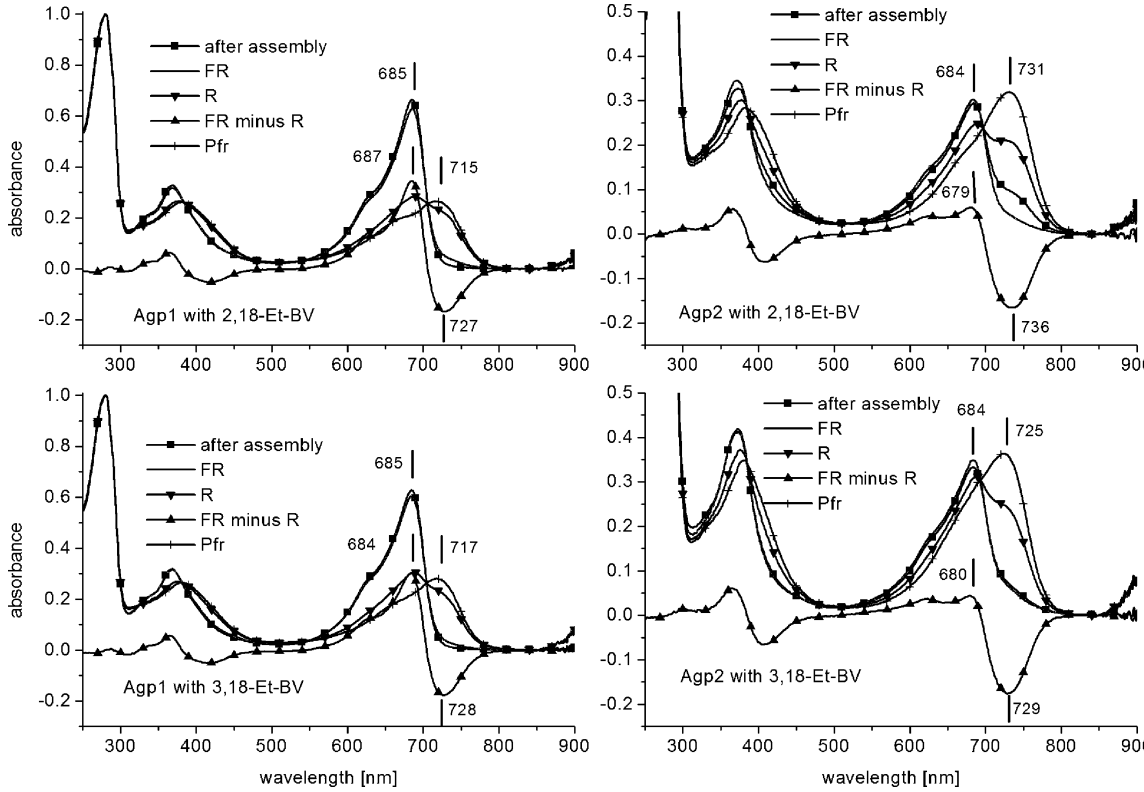

FIGURE 2: UV−vis spectra of Agp1 and Agp2 after the assembly with 2,18-Et-BV or 3,18-Et-BV. Positions of Pr maxima in the absorption and difference spectra in nanometers are given.

with Agp1 and with an N-terminal ca. 500-amino acid truncation fragment of Agp2 (AtBphP2) in previous studies. The chromophore formed a noncovalent, photoreversible adduct with Agp1 (*15*) but did not assemble with the Agp2 (AtBphP2) truncation fragment (*17*). The 2,18-Et-BV chromophore has not been used in previous studies. It should be noted that 2,18-Et-BV and 5*Ea*15*Ea*-BV are symmetrical molecules. All other bilin derivatives used here are not symmetrical. Since there is no covalent link with the protein, the chromophores might enter the chromophore pocket also in a reverse orientation if possible.

In this study, the Agp1 or Agp2 apoprotein samples were always adjusted to an A_{280} of 1, corresponding to a concentration of ca. 10 μM for Agp1 and ca. 12 μM for Agp2. Chromophores were added from stock solutions to final concentrations of either 5 or 10 μM. The shapes of the spectra did not significantly differ between both concentrations; only data from 10 μM are presented here. The assembly was followed by measuring absorption spectra directly after mixing (t = 1 min) and then periodically in given time intervals for up to 2 h. The absorption changes show whether a given chromophore is "accepted" by the protein and give a rough estimation of the kinetics of the assembly process. After the assembly, each sample was passed over a NAP desalting column. Such columns are well suited for the separation of free bilins from the holoprotein.

Adducts with Unlocked Chromophores. The measurements with the 2,18-Et-BV and 3,18-Et-BV control chromophores gave interesting insights into chromophore−protein interaction. Therefore, these data will be described prior to the data that were obtained with the locked chromophores.

We found that both chromophores assembled with Agp1 and Agp2. The maxima in the red spectral region are at 685 nm for both Agp1 adducts and at 684 nm for both Agp2 adducts (Figure 2). The Pr absorption maxima of BV−Agp1 and BV−Agp2 adducts are at 702 and 703 nm, respectively (*18*) (see also Table 1). Adducts with the synthetic 18-Et-BV chromophore, in which the conjugated system of BV is shortened by one double bond, have Pr maxima at 690 and 692 nm, respectively (*18*). Thus, the absorption maxima of the 2,18-Et-BV and 3,18-Et-BV adducts are blue-shifted by 5−8 nm as compared to the Pr form of the 18-Et-BV adducts. This difference is interesting since covalently bound 18-Et-BV has the same number of double bonds in the conjugated system as both noncovalently bound chromophores: during covalent bond formation, either the C3 vinyl group of 18-Et-BV converts to a β-substituted ethyl group (*33*) or it converts to an ethylidene substituent and the C2═C3 bond is lost (*31, 41*). These results point to the latter alternative and indicate that the newly formed ethylidene double bond is "better integrated" in the conjugated system than the C2═C3 bond of the noncovalently bound chromophores, e.g., by a relatively flat structure to make the conjugation more efficient.

For both phytochromes, the assembly with 3,18-Et-BV proceeds significantly faster than that with 2,18-Et-BV. One minute after Agp1 or Agp2 had been mixed with 3,18-Et-BV, absorption changes were almost completed (Figure 3). Similar results have been obtained for the assembly of Agp1 with BV (*22*). With 2,18-Et-BV and Agp1, the absorption increased steadily over the entire tested time range of 120 min, and the assembly of 2,18-Et-BV with Agp2 was completed after 60 min.

The BV−Agp2 adduct converts from Pr to Pfr in darkness, a process which also takes place during the assembly of the chromophores with the protein (*16, 18, 45*). The same

Table 1: Absorption Maxima in the Red Spectral Region (Q-band) of Agp1 and Agp2 Adducts with Photoconvertible Chromophores and Doubly Locked 5*Ea*15*Ea*-BV and 5*Za*15*Ea*-BV[a]

	λ_{max} of Pr (nm)	λ_{max} of Pfr (nm)	λ_{max} of Pr minus Pfr difference spectrum (nm)	λ_{min} of Pr minus Pfr difference spectrum (nm)	λ_{max} of Q-band (nm)
Agp1					
BV from ref *18*	702	748	702	753	
18-Et-BV from ref *18*	690	737	689	741	
2,18-Et-BV	685	715	687	727	
3,18-Et-BV	685	717	684	728	
5*Ea*15*Ea*-BV					698
5*Za*15*Ea*-BV					685
Agp2					
BV from ref *18*	703	760	696	756	
18-Et-BV from ref *18*	692	756	688	745	
2,18-Et-BV	684	731	679	736	
3,18-Et-BV	684	725	680	729	
5*Ea*15*Ea*-BV					700
5*Za*15*Ea*-BV					703

[a] The Pfr spectra of BV−Agp1, 18-Et-BV−Agp1, 2,18-Et-BV−Agp1, 3,18-Et-BV−Agp1, 2,18-Et-BV−Agp2, and 3,18-Et-BV−Agp2 adducts were calculated under the assumption that the relative Pfr content after saturating red irradiation is 0.88, 0.9, 0.83, 0.78, 0.6, and 0.6, respectively. Some of the calculated Pfr spectra are given in Figure 2.

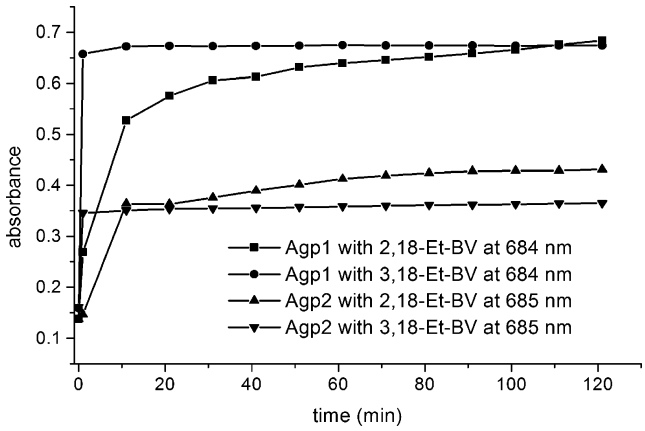

FIGURE 3: Time course of absorbance changes observed upon mixing Agp1 or Agp2 apoprotein with 2,18-Et-BV or 3,18-Et-BV chromophore. The absorbance for time zero was taken from the spectrum of the given chromophore in buffer solution. The other values were taken after the given protein had been mixed with the chromophore.

principle holds for the 18-Et-BV−Agp2 adduct, although dark conversion kinetics are significantly slower (*18*). In contrast, Pr to Pfr dark conversion was not apparent during the assembly of Agp2 with 3,18-Et-BV. The 2,18-Et-BV adduct of Agp2 had a shoulder around 730 nm, which points to the presence of a small fraction of Pfr, but the Pr form predominates. Under far-red illumination, the photoequilibrium of phytochromes is far on the Pr side (typically ca. 95% Pr). When freshly assembled 2,18-Et-BV−Agp2 and 3,18-Et-BV−Agp2 adducts were irradiated with far-red light of 780 nm, the Pr absorption increased and the absorption in the 730 nm range decreased. Thus, the 730 nm shoulder of the freshly assembled 2,18-Et-BV−Agp2 adduct is indeed a Pfr shoulder. The irradiation showed also that the freshly assembled 3,18-Et-BV−Agp2 adduct contains a small fraction of Pfr. When the Agp1 adducts were irradiated with far-red light, the Pr peak was slightly reduced and a subtle increase in the 730 nm region was observed. This result shows that Agp1 adducts are completely in the Pr form after assembly and that far-red (which is absorbed by Pr) light forms a small amount of Pfr. Under red light, the photoequilibrium is on the Pfr side, typically 70−90% Pfr. In all four adducts, the subsequent irradiation with red light resulted in an absorbance increase around 730 nm and a decrease of the Pr peak. The shapes of the Pr minus Pfr difference spectra are comparable to those of the corresponding BV and 18-Et-BV adducts.

Spectra of pure Pfr were calculated from the original data. The Pfr absorption maxima of 2,18-Et-BV−Agp1, 2,18-Et-BV−Agp2, 3,18-Et-BV−Agp1, and 3,18-Et-BV−Agp2 adducts were at 715, 731, 717, and 725 nm, respectively (Figure 2 and Table 1).

These spectral analyses suggest that 2,18-Et-BV−Agp2 and 3,18-Et-BV−Agp2 adducts, unlike BV−Agp2 adducts, convert from Pfr to Pr in darkness or that the extent of their dark conversion from Pr to Pfr is significantly reduced. To determine the principle direction of dark conversion in these adducts, we measured absorbance changes after saturating FR or R irradiation (Figure 4). For both Agp2 adducts, the results were qualitatively similar. When the major fraction was converted to Pfr by red light, Pfr to Pr conversion was observed in the subsequent dark period. When the samples were irradiated with FR to convert the major fraction into Pr, dark conversion from Pr to Pfr was observed. In the control with the BV−Agp2 adduct, Pr to Pfr dark conversion was observed after both irradiations. (Note that after a red light irradiation, a significant fraction is still in the Pr form.) Thus, the mode of chromophore binding (covalent or noncovalent) has a significant impact on the direction of dark conversion of Agp2 adducts.

Assembly with Doubly Locked "5-syn Chromophores," 5Es15Ea-BV and 5Zs15Ea-BV. If an adduct with a doubly locked chromophore is comparable to Pfr, absorption maxima around 715 nm for Agp1 and 731 nm for Agp2 are expected. These rather long wavelengths were not reached for doubly locked chromophores. Moreover, all chromophores in which the single bond of the C5 methine bridge is in the *syn* conformation yielded adducts that absorbed in the blue region only. Spectra that were obtained with these 5-*syn* chromophores 5*Es*15*Ea*-BV and 5*Zs*15*Ea*-BV are presented in Figure 5. In each panel, three spectra are given: (i) that of the chromophore in buffer solution, (ii) that of the chromophore after mixing with protein and completion of assembly, and (iii) that of the same solution after NAP column separation. For the sake of comparison, spectra (ii)

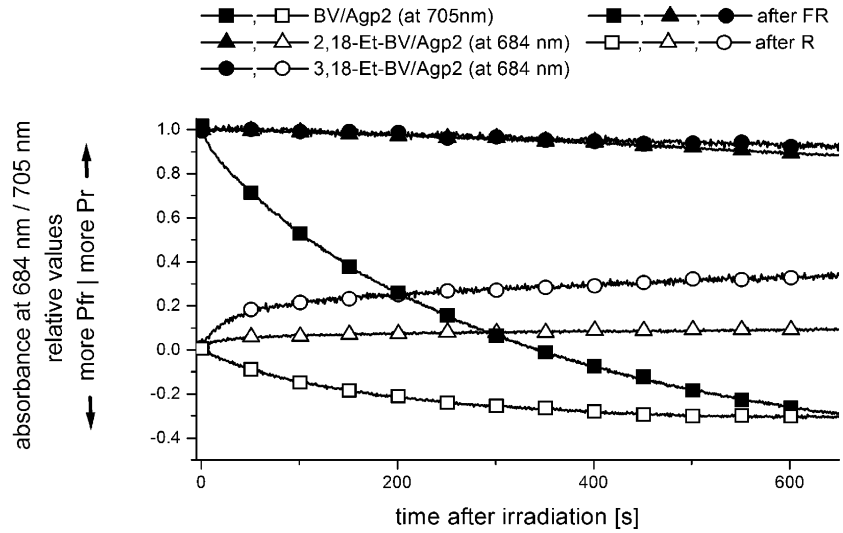

FIGURE 4: Dark conversion of Agp2 adducts after saturating FR or R irradiations. Time course of absorbance changes of BV (squares), 2,18-Et-BV (triangles), or 3,18-Et-BV (circles) adducts after saturation of FR (780 nm) or R (655 nm) irradiations. Absorption was measured at or close to the Pr maximum (705 nm for the BV adduct and 684 nm for 2,18-Et-BV and 3,18-Et-BV adducts). For the sake of comparison, the absorption values after R and FR irradiations of each adduct are set to 0 and 1, respectively. Note that the Pr content of the BV−Agp2 adduct decreases after saturating R irradiation, because residual Pr converts to Pfr in darkness whereas Pfr does not convert to Pr. Net dark conversion of both other adducts after R irradiation proceeds from Pfr to Pr.

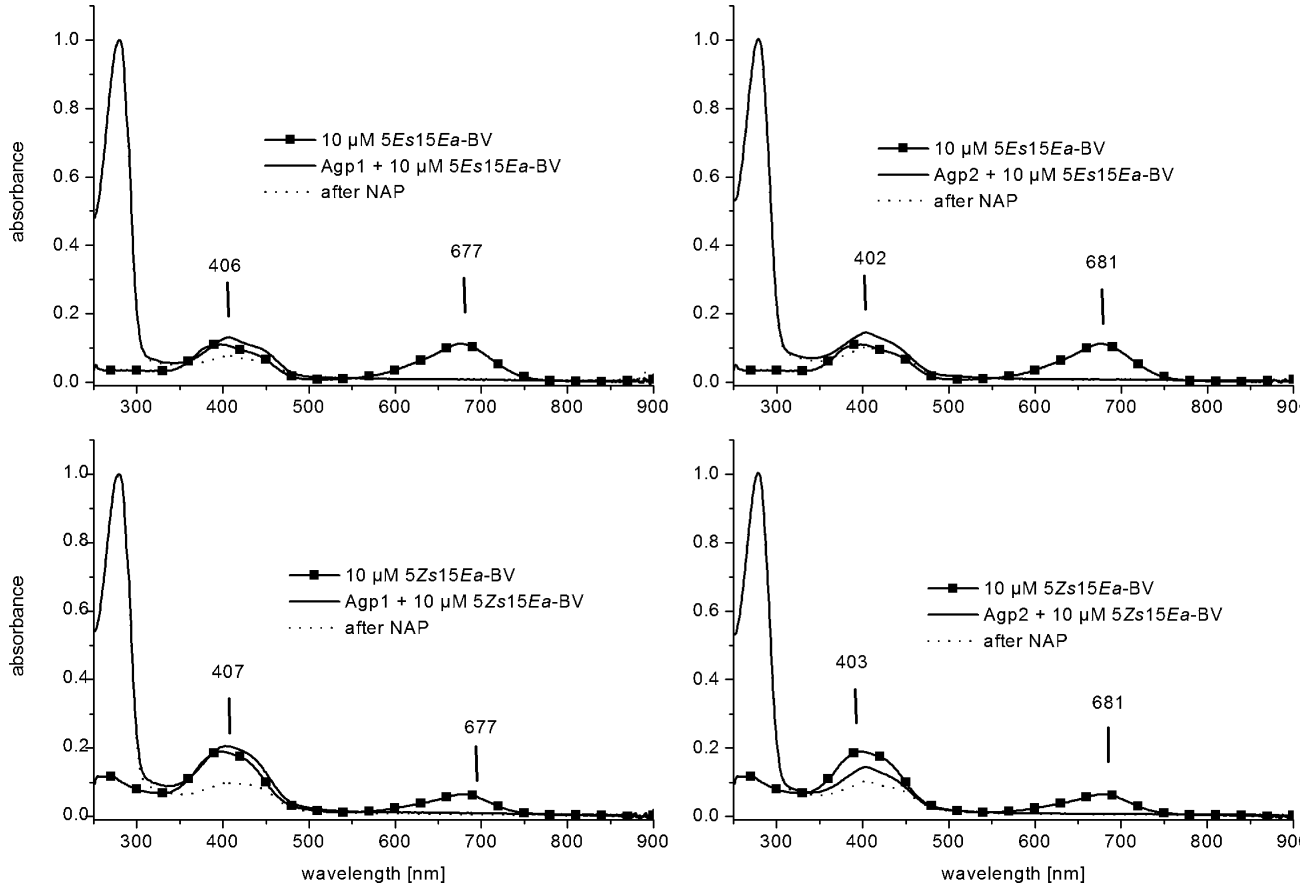

FIGURE 5: Assembly of Agp1 and Agp2 with 5*Es*15*Ea*-BV and 15*Zs*15*Ea*-BV (UV−vis spectra). In each panel, spectra of free chromophores in buffer solution, spectra of the adduct 15 min after mixing protein and chromophore, and spectra of the adduct after NAP column separation are given. Spectra of protein samples are normalized to A_{280}.

and (iii) were normalized to A_{280}, the absorption maximum of the protein. The spectra of both free chromophores in aqueous buffer solution have maxima in the red and blue spectral range, corresponding to the Q-band and Soret band characteristic for typical bilins, respectively. Upon addition of Agp1 or Agp2, the Q-band is lost and only a maximum in the blue spectral range is found. The absorbance changes were already completed when the first spectrum after mixing was measured [$t = 1$ min (Figure 6)]. These data show that both chromophores interact rapidly with Agp1 and Agp2. The complete loss of the Q-band upon assembly of the 5-*syn* chromophores (Figure 5) indicates that all chromophore

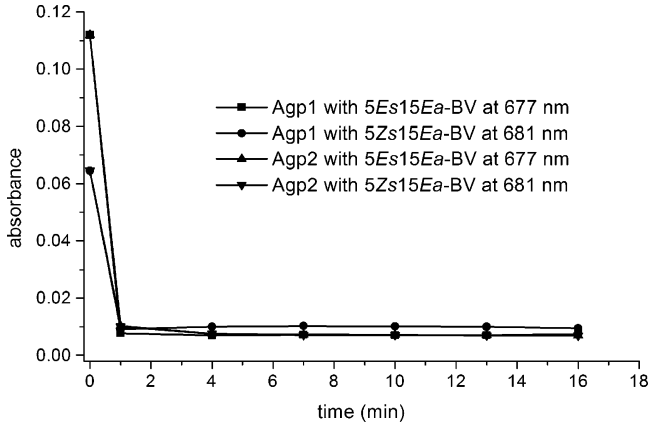

FIGURE 6: Time course of absorbance changes observed upon mixing Agp1 or Agp2 apoprotein with 5*Es*15*Ea*-BV or 5*Zs*15*Ea*-BV. The absorbance for time zero was taken from the spectrum of the given chromophore in buffer solution. The other values were taken after the given protein had been mixed with the chromophore.

Table 2: Absorption Maxima of Adducts with Doubly Locked 5-*syn* Chromophores in Comparison with Absorption Maxima of Adducts with Singly Locked 5- or 15-*syn* Chromophores from a Previous Study

	λ_{max} of adduct (nm)
Agp1	
5*Es*15*Ea*-BV	406
5*Zs*15*Ea*-BV	407
15*Es* from ref *18*	427
15*Zs* from ref *18*	430
photoproduct of 5*Zs* adduct (Pnr form) from ref *18*	636
Agp2	
5*Es*15*Ea*-BV	402
5*Zs*15*Ea*-BV	403
15*Es* from ref *18*	450
15*Zs* from ref *18*	442
photoproduct of 5*Zs* adduct (Pnr form) from ref *18*	675

molecules are incorporated into protein. Upon NAP separation, between 30 and 60% of chromophore is lost (Figure 5). This result indicates that the interaction of the 5-*syn* chromophores with the proteins is weak as compared to the control chromophores, where we observed no loss of chromophore during this treatment (data not shown), or the 5-*anti* chromophores (see below). The loss of the Q-band and the rapid assembly are also characteristic of the singly locked chromophores 15*Es* and 15*Zs*, which form covalent adducts with Agp1 and Agp2 (ref *18* and Table 2).

The absorption spectra of the adducts with 5*Es*15*Ea*-BV, 5*Zs*15*Ea*-BV, 15*Es*, and 15*Zs* are characteristic of dipyrrole systems, which typically have one maximum around 400−460 nm (*46*). Thus, the conjugated system of these chromophores is interrupted by either a kink between pyrrole rings B and C or addition of a nucleophile to the double bond at the C10 position. This interruption leaves two dipyrrole systems with separate conjugated systems, both of which should absorb in the blue spectral range. The half containing rings A and B of the doubly locked 5-*syn* chromophores is identical with the half containing rings C and D of 15*Es* or 15*Zs*. However, the absorption maxima of the adducts with doubly locked chromophores and with singly locked chromophores are 20−48 nm apart from each other (Table 2). We therefore conclude that the absorption maximum of the adducts is determined by the other half of the chromophores, which is the 15*Ea* part of the doubly locked chromophores.

The weak chromophore−protein interaction of the doubly locked 5-*syn* chromophores suggests that only two pyrrole rings are incorporated into the chromophore pocket and that the other two are oriented toward the surface of the protein. The exact geometry can presently not be predicted, but the spectral measurements clearly show that both 5-*syn* chromophores do not represent the Pfr situation. In this sense, the interpretation of the 5*Zs* adducts and photoproducts given above is supported by the doubly locked chromophores.

Assembly with Doubly "Locked 5-anti Chromophores" 5Ea15Ea-BV and 5Za15Ea-BV. Adducts with the doubly locked 5-*anti* chromophores 5*Ea*15*Ea*-BV and 5*Za*15*Ea*-BV absorbed all in the blue and red spectral region (Figure 7). The spectra are presented in the same way as those in Figure 5. Both 5-*anti* chromophores were also incorporated into Agp1 and Agp2 as indicated by spectral changes that took place upon mixing. We noted that in all four cases the assembly is characterized by rapid strong spectral changes that are followed by slower, weaker changes which are not totally completed 2 h after mixing (Figure 8). The free symmetrical 5*Ea*15*Ea*-BV chromophore in buffer solution has maxima at 375 and 607 nm. In the 5*Ea*15*Ea*-BV−Agp1 adduct, there are two maxima in the red and there is one maximum in the blue with a broad shoulder. The shape of this spectrum is unusual for a phytochrome, but the λ_{max} of the red-most peak with 698 nm is positioned between the λ_{max} values of the Pr and Pfr forms of the 2,18-Et-BV−Agp1 adduct (Table 1). Upon NAP column separation, ca. 20% of the chromophore was lost (Figure 7). The 5*Ea*15*Ea*-BV−Agp2 adduct has a strong Q-band and a weaker Soret band. In this respect, the spectrum is similar to that of typical phytochromes, although Agp2 adducts with, for example, 2,18-Et-BV have comparable oscillator strengths in the Soret and Q-band regions (compare Figure 2). The maximum of the Q-band is at 700 nm and thus red-shifted versus the Pr maximum of the 2,18-Et-BV−Agp2 adduct by 16 nm. Upon NAP column separation, the normalized absorption in the Soret band region was unchanged, indicating that there was no loss of chromophore: this chromophore is also tightly bound to the protein. The normalized Q-band absorption increased even slightly after column separation. We assume that the extinction coefficient in this spectral region increases upon interaction of the holoprotein with the column matrix, e.g., because of an improved protein folding.

Free 5*Za*15*Ea*-BV chromophore revealed two maxima in the red and one maximum in the blue spectral range and thus adopts probably two different major conformations around the C10 methine bridge which are present in equal concentrations. The 5*Za*15*Ea*-BV−Agp1 adduct has a typical phytochrome-like spectrum with maxima in the blue and red. The position of the Q-band maximum at 685 nm matches exactly with the Pr form of the 2,18-Et-BV adduct (Table 1). The 5*Za*−Agp1 adduct with a singly locked chromophore has an absorption maximum at 672 nm in the dark-adapted stage; photoconversion produces a red-shifted species (*18*). The calculated spectrum of the pure 5*Za*−Agp1 photoproduct has a maximum at 703 nm (ref *18* and data not shown). Spectra of the 5*Za*15*Ea*-BV−Agp1 adduct and the photoproduct of the 5*Za*−Agp1 adduct are thus dissimilar. We propose two alternative theories to explain this difference. (i) The 5*Za*15*Ea*-BV−Agp1 adduct is a Pfr-like form in which the absorption maximum is shifted to lower wave-

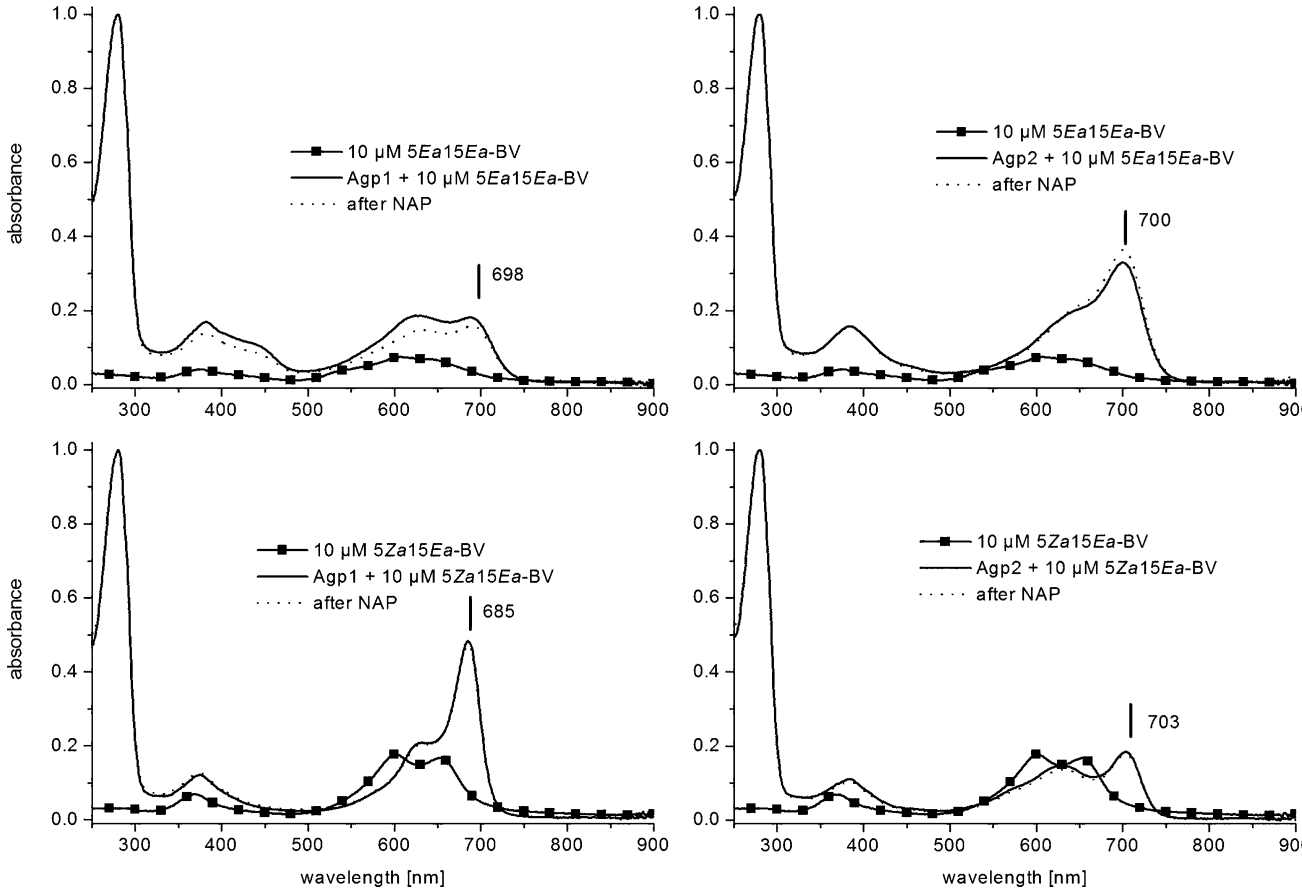

FIGURE 7: Assembly of Agp1 and Agp2 with 5*Ea*15*Ea*-BV and 15*Za*15*Ea*-BV (UV−vis spectra). In each panel, spectra of free chromophores in buffer solution, spectra of the adduct 120 min after mixing protein and chromophore, and spectra of the adduct after NAP column separation are given. Spectra of protein samples are normalized to A_{280}.

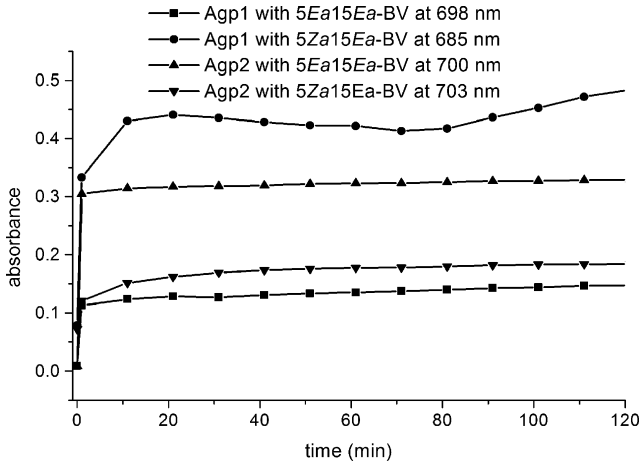

FIGURE 8: Time course of absorbance changes observed upon mixing Agp1 or Agp2 apoprotein with 5*Ea*15*Ea*-BV or 5*Za*15*Ea*-BV. The absorbance for time zero was taken from the spectrum of the given chromophore in buffer solution. The other values were taken after the given protein had been mixed with the chromophore.

lengths because the pyrrole rings are slightly displaced as compared to the natural Pfr chromophore. The discrepancy between the 5*Za*15*Ea*-BV−Agp1 adduct and the 5*Za*−Agp1 photoproduct could be due to the sequence in which rotations around the C15═C16 bond and C5−C6 bond take place: in 5*Za*15*Ea*-BV both rotations are fixed in *E* and *anti*, respectively, before the chromophore enters the pocket, and in the singly locked 5*Za*, the C5−C6 rotation is fixed in the *anti* conformation before the C15═C16 isomerization is induced by irradiation. With the natural chromophore, the C15═C16 isomerization is the first step and the rotation around the C5−C6 bond would follow. (ii) The 5*Za*15*Ea*-BV chromophore might enter the pocket in a reverse manner. In this scenario, it must be regarded as a 5*Ea*15*Za*-BV chromophore, in which the stereochemistry of the C15 methine bridge is Pr-like. The 5*Ea* stereochemistry would not lead to a conflict in the chromophore pocket. NAP column separation showed again that this chromophore is tightly bound to the protein: normalized spectra before and after this separation are almost identical.

Assembly of 5*Za*15*Ea*-BV with Agp2 yields an adduct with two maxima in the red and one in the blue spectral region. The Q-band maximum is positioned at 703 nm, which is the longest wavelength of all adducts with doubly locked chromophores. Also in this case, tight chromophore−protein binding is obtained: normalized spectra before and after NAP separation are identical.

DISCUSSION

In this study, we have assembled *Agrobacterium* apophytochromes Agp1 and Agp2 with synthetic chromophores 3,18-Et-BV, 2,18-Et-BV, 5*Ea*15*Ea*-BV, 5*Es*15*Ea*-BV, 5*Za*15*Ea*-BV, and 5*Zs*15*Ea*-BV (Figure 1). 2,18-Et-BV and 3,18-Et-BV served mainly as control chromophores for the other, doubly locked chromophores. All these bilin derivatives were found to be incorporated into the chromophore pocket of Agp1 or Agp2. Since these compounds have no vinyl side chain at the C3 position of ring A, which is required for the

formation of a covalent link with Cys 20 of Agp1 or Cys 13 of Agp2, the incorporation is noncovalent. It has been shown for Agp1 and other phytochromes that covalent binding is not essential for chromophore assembly and photoconversion. Cys 20 of Agp1 can be blocked with, for example, iodoacetamide or can be replaced by another amino acid. The natural chromophore BV is still incorporated and undergoes reversible Pr to Pfr photoconversion. Moreover, chromophores such as phycocyanobilin, which have different side chains at the C3 position, are incorporated into wild-type Agp1 in a noncovalent manner (*12, 15*).

Here we found also that Agp2 incorporates chromophores that do not form a covalent link with the protein. Our results with 3,18-Et-BV are in contrast to a study in which the same chromophore was tested for assembly with truncated Agp2, termed AtBphP2-N502. In this fragment, the C-terminal histidine kinase domain is missing (*17*). In that case, no chromophore incorporation was observed. The histidine kinase of Agp2 seems thus to play an important role in chromophore assembly. *P. aeruginosa* phytochrome PaBphP, which like Agp2 belongs to the bathy-phytochromes, incorporates 3,18-Et-BV ("meso-BV"), and the adduct is photoactive (*26*).

Moreover, we found that the major part of the Pr adduct which is obtained after the assembly of Agp2 with 2,18-Et-BV or 3,18-Et-BV is stable in darkness. During our observation time, only a small fraction underwent dark conversion into Pfr, in contrast to the BV or 18-Et-BV adducts of Agp2, which undergo complete dark conversion into Pfr under these conditions. After saturating irradiations to achieve either high Pr or Pfr levels, the Agp2 adducts with noncovalently attached chromophores convert from Pr to Pfr or Pfr to Pr in darkness, whereas the BV adduct converts always from Pr to Pfr. Thus, covalent chromophore attachment is required in Agp2 for proper Pr to Pfr dark conversion. We expect that after very long incubation times 2,18-Et-BV−Agp2 and 3,18-Et-BV−Agp2 adducts will reach a stable state in which no more dark conversion takes place. Possibly, the activation energy for both Pr to Pfr and Pfr to Pr transitions is lowered and thus overcome by thermal motions. In this case, the final stable state would be the result of an equilibrium. However, in most phytochromes tested so far, the activation energy for the Pr to Pfr or Pfr to Pr transition or both requires the energy of an absorbed photon.

For the bathy-phytochrome PaBphP, several point mutations have led to inverted dark conversion. For these mutation experiments, amino acids whose function in the wild-type protein is to stabilize ring D of the chromophore in its *Ea* stereochemistry were selected (*32*). The replacement of BV by 18-Et-BV in Agp2 led to decelerated Pr to Pfr dark conversion (*18*). Also here, the interaction between ring D of the chromophore and the protein is affected. In the noncovalently bound chromophores tested here, the interaction between ring A and the protein is affected. Our data show that this interaction also has an impact on dark conversion.

The doubly locked chromophores were designed for studying the stereochemistry of the C5 methine bridge in the Pfr form. Our results with 5*Z*s15*Ea*-BV show that the 5*Zs* stereochemistry, which is predicted for the Pfr form of Cph1 (*35, 39*) and PaBphP (*32*), is unlikely for the Pfr chromophore of Agp1 and Agp2: both 5*Z*s15*Ea*-BV adducts absorb only blue light, indicating that the chromophore is incorporated in a displaced form. The singly locked 5*Zs* and 15*Ea* chromophores assemble with both proteins (and yield Pr-like and Pfr-like spectra, respectively) (*18*). Thus, the fixed C5 or C15 stereochemistry does not impose a restriction per se on the uptake of the chromophore in 5-*syn* or 15-*anti*, but it is the combination of both which results in the mismatch. It is possible that the 5*Z*s15*Ea*-BV chromophore enters the pocket in a reverse manner. In this case, the stereochemistry would be 5*Ea*15*Zs*. This theory is supported by the spectral similarity of the 15*Es*, 15*Zs*, and 5*Z*s15*Ea*-BV adducts (ref *18* and this work) and by the specifically rapid assembly of these chromophores. However, the *Zs* stereochemistry represents the situation of the Pr chromophore at the C5 methine bridge and would thus best fit into the pocket designated for rings A and B of the natural chromophore. Despite the uncertainty with respect to the orientation, we assume that if the 5*Zs* stereochemistry were realized in the Pfr chromophore, either the Agp1 or the Agp2 5*Zs*15*Ea*-BV adduct would have an absorption maximum in the red spectral region. Since the 5*Es15Ea*-BV adducts absorb also in the blue spectral range only, the 5*Es* stereochemistry can also be excluded for the Pfr chromophores of Agp1 and Agp2, following a similar line of reasoning.

Vibrational spectroscopy shows that the chromophore is protonated in the Pr and Pfr form at one of the central nitrogens (*20*). In both 5-*syn* chromophores, the ring B nitrogen is involved in the lock and can therefore not be protonated, but protonation at the ring C nitrogen is possible. A deprotonated bilin chromophore absorbs also in the red spectral range, as long as it is sited in the chromophore pocket (*20*). The fact that both 5-*syn* chromophores absorb in the blue spectral range only cannot result from an improper protonation status.

The 5*Ea* stereochemistry is the most likely arrangement for the Pfr form of Agp2: the spectrum of the 5*Ea*15*Ea*-BV−Agp2 adduct resembles a typical phytochrome spectrum, and the absorption maximum comes close to the expected absorption maximum of the Pfr form. The transition from Pr to Pfr of Agp2 would thus involve a *syn* to *anti* rotation and a *Z* to *E* isomerization around the C5 methine bridge. Both steps most likely occur together in a "Hula-twist isomerization" (*47*), during which the angles between the planes of pyrrole rings A and B would remain constant or only slightly changed. Photoisomerization of the Hula-twist type has been proposed for retinal chromophores in bacteriorhodopsin and visual rhodopsin and various organic chromophores in solids (*47*). On the basis of NMR data, it has been proposed that the cyanobacterial phytochrome Cph1 might undergo a Hula-twist isomerization around the C5 methine bridge (*38*).

Agp1 spectra leave two options for the Pfr chromophore of this phytochrome. The 5*Ea*15*Ea*-BV adduct has two peaks in the red spectral range. The red-most peak has a maximum at 700 nm, which comes close to the Pfr maximum of the control adduct (715 nm). Thus, the Pfr chromophore of Agp1 could also have a 5*Ea* stereochemistry, leading to the same implications described above for Agp2. However, the spectrum of the 5*Za*15*Ea*-BV−Agp1 adduct looks more typical for a phytochrome and reveals a higher extinction coefficient as compared to that of the 5*Ea*15*Ea*-BV−Agp1

adduct. This adduct has a maximum at 685 nm, 30 nm shorter than that of the Pfr form of the control adduct. In this respect, there is an analogy with the 5*Ea*15*Ea*-BV−Agp2 adduct, which has an absorption maximum 31 nm shorter than that of the Pfr form of the control adduct (731 nm). The shape of the spectrum of the 5*Za*15*Ea*-BV−Agp1 adduct led us to consider that the Pfr chromophore of Agp1 has a 5*Za* stereochemistry. This stereochemistry requires a *syn* to *anti* rotation upon Pr to Pfr conversion.

It could be that the stereochemistry of Agp1 and Agp2 Pfr chromophores differs and that both are also different from other phytochromes, for which a 5*Zs* stereochemistry has been proposed. Although different phytochromes were originally regarded as very similar molecules with similar reaction mechanisms, detailed comparisons showed that phytochromes differ significantly, e.g., with respect to photoconversion kinetics, dark conversion, chromophore protonation and deprotonation, spectral properties, etc. Protein domains are often arranged in the same manner, but the primary structures may differ drastically between the different phytochromes. It might be likely that one common phenomenon, the bathochromic shift upon Pr to Pfr photoconversion, is realized by different mechanisms. A more detailed comparison of different phytochromes with methods employing locked chromophores (e.g., doubly locked chromophores which form a covalent link with the protein), NMR, vibrational spectroscopy, and protein crystallography will complete our understanding in this respect.

We think it is unlikely that the proposed changes of C5 stereochemistry are direct events of light excitation, since there is little doubt that the C15═C16 isomerization is the first, light-driven process for Pr to Pfr conversion in all phytochromes. Thus, the changes around the C5 methine bridge are not directly driven by light but rather by protein and chromophore constraints and subsequent conformational changes in the protein, which are triggered by the first C15 *Z* to *E* reaction.

ACKNOWLEDGMENT

We thank Norbert Michael and Sybille Wörner for help on the purification of Agp1 and Agp2.

REFERENCES

1. Kendrick, R. E., and Kronenberg, G. H. M. (1994) in *Photomorphogenesis in Plants* (Kendrick, R. E., and Kronenberg, G. H. M., Eds.) 2nd ed., Kluwer Academic Publishers, Dordrecht, The Netherlands.
2. Schäfer, E., and Nagy, F. (2006) *Photomorphogenesis in plants and bacteria*, 3rd ed., Springer-Verlag, Berlin.
3. Lagarias, J. C., and Rapoport, H. (1980) Chromopeptides from phytochrome. The structure and linkage of the Pr form of the phytochrome chromophore. *J. Am. Chem. Soc. 102*, 4821–4828.
4. Rockwell, N. C., Su, Y. S., and Lagarias, J. C. (2006) Phytochrome structure and signaling mechanisms. *Annu. Rev. Plant Biol. 57*, 837–858.
5. Vierstra, R., and Karniol, B. (2005) Phytochromes in Microorganisms. In *Handbook of Photosensory Receptors* (Briggs, W. R., and Spudich, J. L., Eds.) pp 171−195, Wiley-Verlag, Weinheim, Germany.
6. Lamparter, T. (2004) Evolution of cyanobacterial and plant phytochromes. *FEBS Lett. 573*, 1–5.
7. Blumenstein, A., Vienken, K., Tasler, R., Purschwitz, J., Veith, D., Frankenberg-Dinkel, N., and Fischer, R. (2005) The *Aspergillus nidulans* phytochrome FphA represses sexual development in red light. *Curr. Biol. 15*, 1833–1838.
8. Bhoo, S. H., Davis, S. J., Walker, J., Karniol, B., and Vierstra, R. D. (2001) Bacteriophytochromes are photochromic histidine kinases using a biliverdin chromophore. *Nature 414*, 776–779.
9. Lamparter, T. (2006) A computational approach to discovering the functions of bacterial phytochromes by analysis of homolog distributions. *BMC Bioinf. 7*, 141.
10. Quest, B., Hübschmann, T., Sharda, S., Tandeau, d. M., and Gärtner, W. (2007) Homologous expression of a bacterial phytochrome. The cyanobacterium *Fremyella diplosiphon* incorporates biliverdin as a genuine, functional chromophore. *FEBS J. 274*, 2088–2098.
11. Hübschmann, T., Börner, T., Hartmann, E., and Lamparter, T. (2001) Characterisation of the Cph1 holo-phytochrome from *Synechocystis* sp. PCC 6803. *Eur. J. Biochem. 268*, 2055–2063.
12. Lamparter, T., Michael, N., Mittmann, F., and Esteban, B. (2002) Phytochrome from *Agrobacterium tumefaciens* has unusual spectral properties and reveals an N-terminal chromophore attachment site. *Proc. Natl. Acad. Sci. U.S.A. 99*, 11628–11633.
13. Lamparter, T., Carrascal, M., Michael, N., Martinez, E., Rottwinkel, G., and Abian, J. (2004) The biliverdin chromophore binds covalently to a conserved cysteine residue in the N-terminus of *Agrobacterium phytochrome* Agp1. *Biochemistry 43*, 3659–3669.
14. Elich, T. D., and Chory, J. (1997) Biochemical characterization of *Arabidopsis* wild-type and mutant phytochrome B holoproteins. *Plant Cell 9*, 2271–2280.
15. Lamparter, T., Michael, N., Caspani, O., Miyata, T., Shirai, K., and Inomata, K. (2003) Biliverdin binds covalently to *Agrobacterium* phytochrome Agp1 via its ring A vinyl side chain. *J. Biol. Chem. 278*, 33786–33792.
16. Karniol, B., and Vierstra, R. D. (2003) The pair of bacteriophytochromes from *Agrobacterium tumefaciens* are histidine kinases with opposing photobiological properties. *Proc. Natl. Acad. Sci. U.S.A. 100*, 2807–2812.
17. Karniol, B., Wagner, J. R., Walker, J. M., and Vierstra, R. D. (2005) Phylogenetic analysis of the phytochrome superfamily reveals distinct microbial subfamilies of photoreceptors. *Biochem. J. 392*, 103–116.
18. Inomata, K., Noack, S., Hammam, M. A. S., Khawn, H., Kinoshita, H., Murata, Y., Michael, N., Scheerer, P., Krauss, N., and Lamparter, T. (2006) Assembly of synthetic locked chromophores with *Agrobacterium* phytochromes Agp1 and Agp2. *J. Biol. Chem. 281*, 28162–28173.
19. Inomata, K., Hammam, M. A. S., Kinoshita, H., Murata, Y., Khawn, H., Noack, S., Michael, N., and Lamparter, T. (2005) Sterically locked synthetic bilin derivatives and phytochrome Agp1 from *Agrobacterium tumefaciens* form photoinsensitive Pr- and Pfr-like adducts. *J. Biol. Chem. 280*, 24491–24497.
20. Borucki, B., von Stetten, D., Seibeck, S., Lamparter, T., Michael, N., Mroginski, M. A., Otto, H., Murgida, D. H., Heyn, M. P., and Hildebrandt, P. (2005) Light-induced proton release of phytochrome is coupled to the transient deprotonation of the tetrapyrrole chromophore. *J. Biol. Chem. 280*, 34358–34364.
21. von Stetten, D., Seibeck, S., Michael, N., Scheerer, P., Mroginski, M. A., Murgida, D. H., Krauss, N., Heyn, M. P., Hildebrandt, P., Borucki, B., and Lamparter, T. (2007) Highly conserved residues D197 and H250 in Agp1 phytochrome control the proton affinity of the chromophore and Pfr formation. *J. Biol. Chem. 282*, 2116–2123.
22. Noack, S., Michael, N., Rosen, R., and Lamparter, T. (2007) Protein conformational changes of *Agrobacterium* phytochrome Agp1 during chromophore assembly and photoconversion. *Biochemistry 46*, 4164–4176.
23. Schumann, C., Gross, R., Wolf, M. M., Diller, R., Michael, N., and Lamparter, T. (2008) Subpicosecond midinfrared spectroscopy of the Pfr reaction of phytochrome Agp1 from *Agrobacterium tumefaciens*. *Biophys. J. 94*, 3189–3197.
24. Krieger, A., Molina, I., Oberpichler, I., Michael, N., and Lamparter, T. (2008) Spectral properties of phytochrome Agp2 from *Agrobacterium tumefaciens* are specifically modified by a compound of the cell extract. *J. Photochem. Photobiol., B 93*, 16–22.
25. Giraud, E., Fardoux, J., Fourrier, N., Hannibal, L., Genty, B., Bouyer, P., Dreyfus, B., and Vermeglio, A. (2002) Bacteriophytochrome controls photosystem synthesis in anoxygenic bacteria. *Nature 417*, 202–205.
26. Tasler, R., Moises, T., and Frankenberg-Dinkel, N. (2005) Biochemical and spectroscopic characterization of the bacterial phytochrome of *Pseudomonas aeruginosa*. *FEBS J. 272*, 1927–1936.
27. von Stetten, D., Gunther, M., Scheerer, P., Murgida, D. H., Mroginski, M. A., Krauss, N., Lamparter, T., Zhang, J., Anstrom,

D. M., Vierstra, R. D., Forest, K. T., and Hildebrandt, P. (2008) Chromophore heterogeneity and photoconversion in phytochrome crystals and solution studied by resonance Raman spectroscopy. *Angew. Chem., Int. Ed. 47*, 4753–4755.
28. Mroginski, M. A., Murgida, D. H., von Stetten, D., Kneip, C., Mark, F., and Hildebrandt, P. (2004) Determination of the chromophore structures in the photoinduced reaction cycle of phytochrome. *J. Am. Chem. Soc. 126*, 16734–16735.
29. Foerstendorf, H., Lamparter, T., Hughes, J., Gärtner, W., and Siebert, F. (2000) The photoreactions of recombinant phytochrome from the cyanobacterium *Synechocystis*: A low-temperature UV-Vis and FT-IR spectroscopic study. *Photochem. Photobiol. 2000*, 655–661.
30. Vogel, R., and Siebert, F. (2000) Vibrational spectroscopy as a tool for probing protein function. *Curr. Opin. Chem. Biol. 4*, 518–523.
31. Yang, X., Stojkovic, E. A., Kuk, J., and Moffat, K. (2007) Crystal structure of the chromophore binding domain of an unusual bacteriophytochrome, RpBphP3, reveals residues that modulate photoconversion. *Proc. Natl. Acad. Sci. U.S.A. 104*, 12571–12576.
32. Yang, X., Kuk, J., and Moffat, K. (2008) Crystal structure of *Pseudomonas aeruginosa* bacteriophytochrome: Photoconversion and signal transduction. *Proc. Natl. Acad. Sci. U.S.A. 105*, 14715–14720.
33. Wagner, J. R., Brunzelle, J. S., Forest, K. T., and Vierstra, R. D. (2005) A light-sensing knot revealed by the structure of the chromophore-binding domain of phytochrome. *Nature 438*, 325–331.
34. Essen, L. O., Mailliet, J., and Hughes, J. (2008) The structure of a complete phytochrome sensory module in the Pr ground state. *Proc. Natl. Acad. Sci. U.S.A. 105*, 14709–14714.
35. Hahn, J., Strauss, H. M., and Schmieder, P. (2008) Heteronuclear NMR Investigation on the Structure and Dynamics of the Chromophore Binding Pocket of the Cyanobacterial Phytochrome Cph1. *J. Am. Chem. Soc. 130*, 11170–11178.
36. Rohmer, T., Strauss, H., Hughes, J., de Groot, H., Gärtner, W., Schmieder, P., and Matysik, J. (2006) ^{15}N MAS NMR studies of Cph1 phytochrome: Chromophore dynamics and intramolecular signal transduction. *J. Phys. Chem. B 110*, 20580–20585.
37. Strauss, H. M., Hughes, J., and Schmieder, P. (2005) Heteronuclear solution-state NMR studies of the chromophore in cyanobacterial phytochrome Cph1. *Biochemistry 44*, 8244–8250.
38. van Thor, J. J., Mackeen, M., Kuprov, I., Dwek, R. A., and Wormald, M. R. (2006) Chromophore structure in the photocycle of the cyanobacterial phytochrome Cph1. *Biophys. J. 91*, 1811–1822.
39. Rohmer, T., Lang, C., Hughes, J., Essen, L. O., Gärtner, W., and Matysik, J. (2008) Light-induced chromophore activity and signal transduction in phytochromes observed by ^{13}C and ^{15}N magic-angle spinning NMR. *Proc. Natl. Acad. Sci. U.S.A. 105*, 15229–15234.
40. Seibeck, S., Borucki, B., Otto, H., Inomata, K., Khawn, H., Kinoshita, H., Michael, N., Lamparter, T., and Heyn, M. P. (2007) Locked 5Zs-biliverdin blocks the Meta-R_A to Meta-R_C transition in the functional cycle of bacteriophytochrome Agp1. *FEBS Lett. 581*, 5425–5429.
41. Wagner, J. R., Zhang, J., Brunzelle, J. S., Vierstra, R. D., and Forest, K. T. (2007) High resolution structure of *Deinococcus* bacteriophytochrome yields new insights into phytochrome architecture and evolution. *J. Biol. Chem. 282*, 12298–12309.
42. Rüdiger, W., Thümmler, F., Cmiel, E., and Schneider, S. (1983) Chromophore structure of the physiologically active form (Pfr) of phytochrome. *Proc. Natl. Acad. Sci. U.S.A. 80*, 6244–6248.
43. Khawn, H., Chen, L.-Y., Kinoshita, H., and Inomata, K. (2008) Total syntheses of doubly locked biliverdin derivatives toward elucidation of the stereochemistry of phytochrome chromophore. *Chem. Lett. 37*, 198–199.
44. Inomata, K. (2008) Studies on the structure and function of phytochromes as photoreceptors based on synthetic organic chemistry. *Bull. Chem. Soc. Jpn. 81*, 25–59.
45. Lamparter, T., and Michael, N. (2005) *Agrobacterium* phytochrome as an enzyme for the production of ZZE bilins. *Biochemistry 44*, 8461–8469.
46. Falk, H. (1989) *The chemistry of linear oligopyrroles and bile pigments*, Springer-Verlag, Berlin.
47. Liu, R. S. (2001) Photoisomerization by hula-twist: A fundamental supramolecular photochemical reaction. *Acc. Chem. Res. 34*, 555–562.

BI802334U